Variations in the torsion-vibration energy structure of CH_3OH from fundamental, overtone, and combination bands of the ν_7, ν_8, and ν_{11} CH_3 rocking and CO stretching modes

R. M. Lees,[1,*] M. Mollabashi,[2] Li-Hong Xu,[3] M. Lock,[4] and B. P. Winnewisser[4,5]
[1]*Department of Physics, University of New Brunswick, Fredericton, New Brunswick, Canada E3B 5A3*
[2]*Department of Physics, Iran University of Science and Technology, Narmak, Tehran 16844, Iran*
[3]*Department of Physical Sciences, University of New Brunswick, Saint John, New Brunswick, Canada E2L 4L5*
[4]*Physikalisch-chemisches Institut, Justus-Liebig-Universität, Heinrich-Buff-Ring 58, D-35392 Giessen, Germany*
[5]*Department of Physics, The Ohio State University, 174 West 18th Avenue, Columbus, Ohio 43210*
(Received 11 January 2002; published 5 April 2002)

Torsion-vibration energy structures deduced from the ν_7 (A' CH_3 in-plane rocking mode), ν_8 (A' CO stretching mode), ν_{11} (A'' CH_3 out-of-plane rocking mode), $2\nu_7$, $2\nu_8$, $\nu_7+\nu_8$, and $\nu_8+\nu_{11}$ fundamental, overtone, and combination bands of CH_3OH are compared and contrasted to that of the ground vibrational state. The $2\nu_7$ in-plane CH_3-rocking overtone and the $\nu_8+\nu_{11}$ CO-stretching and out-of-plane rocking combination bands are identified in the high-resolution Fourier transform spectrum, and point to systematic trends in the excited-state torsional behavior for methanol. Torsion-vibration substate origins have been determined for the eight modes considered, and fitted to a five-parameter Fourier model to characterize the energy patterns. Excitation of the ν_8 mode has little influence on the torsional structure, but the *A-E* torsional energy splittings are sharply reduced with excitation of ν_7 and inverted with excitation of ν_{11}. These changes are examined from the perspective of a recent torsion-vibration interaction model for states of degenerate *E* vibrational parentage [J. T. Hougen, J. Mol. Spectrosc. **207**, 60 (2001)]; the $K=0$ substate energy pattern for ν_7 and ν_{11} supports Hougen's model but with some differences in detail. The values of the *K*-scaling parameter ρ determining the periodicity of the torsional energies appear to vary almost linearly with the number of quanta of vibrational excitation. The changes are suggestive of substantial zero-point effects on the axial moments of inertia, with implications for the structural determination of the CH_3 methyl top.

DOI: 10.1103/PhysRevA.65.042511 PACS number(s): 33.20.Ea, 33.15.Hp, 33.20.Vq

I. INTRODUCTION

In this paper, we examine interesting and sometimes dramatic variations in the torsion-vibration energy structures of a group of eight fundamental, overtone, and combination states (including the ground state) of the three lowest vibrational modes of CH_3OH, namely, the A' CO-stretching mode (ν_8), the A' in-plane CH_3 rocking mode (ν_7) and the A'' out-of-plane CH_3 rocking mode (ν_{11}). The $n=0$ ground torsional energy curves for each state can be fitted to obtain two important parameters: the torsional *A-E* energy splitting at $K=0$, which gives insight into the potential barrier to internal rotation, and the *K*-scaling parameter ρ which determines the periodicity of the curves and is sensitive to the axial moments of inertia of the CH_3 top and the OH framework. The relatively large-amplitude rocking motions of the light CH_3 group might be expected to have significant effects on both of these terms for states in which the ν_7 or ν_{11} modes are excited, and this is indeed found to be the case.

The ν_8 CO stretching fundamental has been extensively studied in the past, and earlier results and references are reviewed in the book by Moruzzi *et al.* [1]. The $2\nu_8$ overtone has been investigated as well [2–5], and the pattern of the excited-state torsional energies was recently reported together with that for the $\nu_7+\nu_8$ combination band [5]. Results are also known for the ν_7 fundamental for normal CH_3OH [6] and for the $^{13}CD_3OH$ [7], O-18 [8], and C-13 [9] isotopic species. All of the isotopomers show a large increase in effective torsional barrier with excitation of the ν_7 mode. The ν_{11} out-of-plane CH_3 rocking fundamental was investigated not long ago [10], and the ν_{11} *A-E* splitting was found to be inverted relative to the ground state. This inversion is incompatible with the usual one-dimensional large-amplitude Hamiltonian describing the torsional energies alone [11]. However, a recent "$E\times E$" analysis by Hougen [12] has shown for excited vibrational states of *E* parentage, such as the two CH_3 rocking modes, that a wide variety of torsional splitting patterns is possible, including inversion, depending on the relative magnitudes of certain torsion-vibration interaction terms. Thus, one of the incentives for the present paper was to test the $E\times E$ model utilizing our rocking-mode data.

In this paper, we first report observation of new $n=0$ subbands assigned to the $2\nu_7$ overtone and $\nu_8+\nu_{11}$ combination bands of CH_3OH, both of which are important in exploring the systematics of the torsion-vibration energy structures for methanol. The upper-state torsional energies are described in terms of substate origins determined by fitting the excited-state term values to series expansions in powers of $J(J+1)$. The overall picture for the eight currently known vibrational states involving the CO stretching and/or CH_3 rocking modes is then reviewed from the per-

*Author to whom correspondence should be addressed: Physical Sciences Department, University of New Brunswick, Tucker Park, Saint John, N.B., Canada E2L 4L5; FAX: 1-506-648-5948; email address: lees@unb.ca

TABLE I. Vibrational substate W_0 origins and effective B values (in cm^{-1}) for the $2\nu_7$ in-plane CH_3-rocking overtone and the $\nu_8+\nu_{11}$ CO-stretching and out-of-plane rocking combination band of CH_3OH.[a]

Substate	$\tau=1$			$\tau=2$			$\tau=3$		
K	TS	W_0	B_{eff}	TS	W_0	B_{eff}	TS	W_0	B_{eff}
$2\nu_7$ Overtone									
0	A	2273.245	0.8006						
1	E_2	2276.854[b]	0.8003[b]	E_1	2279.516[b]	0.8004[b]	A	2277.804[b,c]	0.8005[b,c]
2	E_1	2287.628[b]	0.8008[b]	A	2290.069[b,c]	0.8008[b,c]	E_2	2287.665[b]	0.8007[b]
3	A	2305.562[b,c]	0.8007[b,c]	E_2	2306.951[b]	0.8005[b]	E_1	2304.207[b]	0.8009[b]
4	E_2	2330.143[b]	0.8008[b]	E_1	2330.274[b]	0.8011[b]	A	2328.070[b,c]	0.8000[b,c]
5	E_1	2361.570	0.8012	A	2360.070	0.8049	E_2	2358.836	0.8027
6	A	2399.048	0.8140	E_2	2395.768	0.7988	E_1	2397.541	0.7850
7	E_2	2443.736	0.7982	E_1	2441.010	0.7990	A	2442.389	0.7977
8	E_1	2494.511	0.7980	A	2492.113	0.7955			
9	A	2551.669	0.7987	E_2	2550.250	0.7987	E_1	2543.649	0.7981
10							A	2618.308	0.7975
$\nu_8+\nu_{11}$ Combination									
4							A	2373.340[c]	0.7942[c]
5				A	2397.274	0.7938			
6	A	2432.491	0.7940						
7							A	2484.323	0.7941

[a]The J-reduced vibrational substate origins and effective B values were obtained from $J(J+1)$ power-series fits to upper state term values which were determined by adding ground-state energies from Ref. [1] to the experimental subband wave numbers.
[b]Average of results from $\Delta K=+1$ and $\Delta K=-1$ subbands accessing the same upper substate.
[c]Average of results from resolved A^+ and A^- subbands.

spective of a simple Fourier model for the $n=0$ K-reduced torsion-vibration energies which yields the $K=0$ A-E torsional splittings and the ρ periodicity parameters. Certain consistent trends are found for the behavior of the various vibrational states, as well as some significant differences. Last, the pattern of the $K=0$ energies and A-E splittings for the two CH_3 rocking modes is examined from the perspective of the Hougen $E\times E$ model.

II. EXPERIMENT

The experimental conditions for the recording of the $2\nu_7$ and $\nu_8+\nu_{11}$ bands of CH_3OH investigated in this paper were described previously [5]. Briefly, Fourier transform infrared spectra were obtained at 0.0048 cm^{-1} resolution (1/MOPD) on the Bruker IFS 120 instrument in the Giessen laboratory. One spectrum was taken at a mean pressure of 256 Pa with 471 scans coadded, and a second at a mean pressure of 52 Pa with 561 scans coadded, both employing a path length of 19.5 m in a White cell operated at room temperature. Calibration against a group of CO line standards in the 2100 cm^{-1} region [13] gave an rms error in (calibrated-standard) CO wave numbers of 0.000 004 9 cm^{-1}, representing the statistical uncertainty in a calibrated measurement.

III. SUBBAND ASSIGNMENTS FOR THE $2\nu_7$ AND $\nu_8+\nu_{11}$ BANDS

The $2\nu_7$ CH_3 rocking overtone band, though weak, displays rich spectral structure over a broad region from about 2100 to 2200 cm^{-1}. The band is of hybrid a/b character, with both parallel $\Delta K=0$ and perpendicular $\Delta K=\pm1$ subbands. (K is the quantum number for the component of the rotational angular momentum along the a axis of internal rotation, taken as parallel to the axis of the three-fold internal top.) However, the parallel subbands are significantly weaker than the perpendicular subbands and, because the torsional structure is quite different in the upper and lower states, the $\Delta K=0$ subband origins are distributed over a relatively wide range. Thus, the typical parallel band contour with a sharp Q branch is not visible in the low-resolution spectrum shown in Fig. 1 of Ref. [5]. (A number of the $\Delta K=+1$ Q subbranches can be seen as small peaks towards the high-frequency side of that spectrum, however.) The initial breakthrough in assignments was for $\Delta K=+1$ subbands of medium K, through their relatively strong R subbranches. The matching $\Delta K=-1$ subbands were then found using ground-state combination differences, and subsequently the weaker $\Delta K=0$ subbands were similarly located. For low K, the Q subbranches of the $\Delta K=-1$ subbands also appear as distinctive features in the spectrum and gave major clues to the assignments.

Upper-state energy term values were calculated from the $\Delta K=\pm1$ subbands by adding known ground-state energies [1] to the subband wave numbers. These term values were then fitted to series expansions in powers of $J(J+1)$ in order to obtain the J-independent substate origins, W_0. The latter are presented in Table I, together with the effective upper-state B values [the coefficients of $J(J+1)$ in the series expansions]. The term values derived from the $\Delta K=-1$ and

TABLE II. Molecular parameters and calculated $K=0$ *A-E* splittings (E_E-E_A) from Fourier fits to $n=0$ torsion-vibration substate origins of CH_3OH.

Vibrational State	E_{vib} (cm^{-1})	a_1 (cm^{-1})	a_2 (cm^{-1})	$[A-(B+C)/2]$ (cm^{-1})	ρ	*A-E* Splitting (cm^{-1})
0[a]	134.173	−6.2193	0.2223	3.4399	0.81042	8.996
ν_8	1168.064	−5.7312	0.2160	3.4472	0.80962	8.273
ν_7	1205.909	−3.2481	0.1759	3.4286	0.78144	4.608
ν_{11}	1287.143	5.3140	−0.3108	3.4605	0.79024	−7.505
$2\nu_8$	2188.887	−5.8342	0.1010	3.4549	0.80889	8.600
$\nu_7+\nu_8$	2231.499	−3.1394	0.0402	3.4354	0.77997	4.649
$2\nu_7$	2274.770	−1.5700	0.0437	3.4193	0.75079	2.290
$\nu_8+\nu_{11}$	2313.669	5.1242	0 (fixed)	3.4260	0.78916	−7.686

[a]Accurate parameter values for the ground state obtained from detailed modeling [16] or term value analysis [1] are $E_{vib}=134.057\ cm^{-1}$, $[A-(B+C)/2]=3.4489\ cm^{-1}$, $\rho=0.810\,21$, and *A-E* splitting $=9.122\ cm^{-1}$.

$\Delta K=+1$ subbands were fitted separately, as were the A^+ and A^- components for subbands with resolved asymmetry splittings. The values listed in Table I are the averages of the independent fits, which were very close in all cases.

At a higher wave number in the spectrum, we identified four further subbands of *A* torsional symmetry which did not appear to be associated with $2\nu_7$. The subband origins are consistent with the $\nu_8+\nu_{11}$ CO stretching and out-of-plane rocking mode combination band. This is expected to be weak but, like the $\nu_7+\nu_8$ combination band, can borrow intensity with the ν_{11} component riding on the strong ν_8 CO stretch. The substate origins and effective *B* values derived from the four subbands are given in the bottom section of Table I.

IV. *K*-REDUCED ENERGY τ CURVES AND FOURIER FITS

The interesting thing now is to compare the $n=0$ torsion-vibration energy structures for all of the eight known methanol vibrational states involving excitation of the ν_7, ν_8, and/or ν_{11} modes (including the ground state). An informative way of representing the energy structures is in terms of Burkhard and Dennison's periodic τ curves [14] of *K*-reduced energies, as was discussed previously [5,10]. The *K*-reduced energy, defined as $W_0-[A-(B+C)/2]K^2$, is equal to the substate origin minus the *K*-rotational energy. The symmetry index τ (=1, 2, or 3) specifies the torsional symmetry (TS) according to the rule $(\tau+K)=3N+1$, $3N$, or $3N-1$ for *A*, E_1, and E_2 symmetries, respectively, where *N* is an integer. In Burkhard and Dennison's model, the torsional energies of given τ are oscillatory functions of a variable $(1-\rho)K$, with $\rho\approx I_{CH_3}/I_a$, where I_{CH_3} is the axial moment of inertia of the methyl top and I_a is that of the entire molecule [14]. The $\tau=1$ curve is symmetric about the origin, $(1-\rho)K=0$, while the $\tau=2$ and $\tau=3$ curves are identical in shape but are shifted along the $(1-\rho)K$ axis by -1 and $+1$, respectively. For $K=0$, the traditional one-dimensional Hamiltonian [11] always puts the $\tau=1$ *A* energy below the degenerate $\tau=2/\tau=3$ *E* energy for the $n=0$ torsional ground state, with the *A-E* ordering then alternating with *n* for higher torsional states.

Since the τ curves oscillate with period 3 along the $(1-\rho)K$ axis, the substate origins for vibrational state v can conveniently be represented by a simple five-parameter Fourier model [10,15]

$$W_0^v(K)=E_{vib}^v+a_0^v+a_1^v\cos\{[(1-\rho)K+\tau-1]2\pi/3\}+a_2^v\cos\{[(1-\rho)K+\tau-1]4\pi/3\}+[A-(B+C)/2]^vK^2 \quad (1)$$

where $(E_{vib}^v+a_0^v)$ is a constant including both purely vibrational and zero-point torsional energies, and a_1^v and a_2^v are Fourier coefficients. Accordingly, we fitted $n=0$ substate origins for the eight vibrational states to Eq. (1) using the Solver function in Microsoft Excel spreadsheets. The coefficients obtained and the calculated $K=0$ *A-E* splittings are shown in Table II. We then used the fitted values of the $[A-(B+C)/2]^v$ *K*-rotational constants in order to subtract the *K*-rotational energy from the W_0^v substate origins to obtain "experimental" *K*-reduced energies for our eight states. Figures 1(a)–1(h) show these energies as the plotted points, together with continuous curves calculated from the Fourier model using the constants in Table II. Substates omitted from the fits due to significant perturbations include the $(n\tau K)^v$ $TS=(010)^{co}$ *A* and $(035)^{co}E_2$ ν_8 CO stretching mode origins, both shifted by well-known Fermi resonances with nearby $n=3$ and $n=4$ torsional levels of the ground state [17], the three $K=6$ states for the $2\nu_7$ in-plane rocking overtone, all of which appear to be perturbed, and the $(037)^{ro}$ *A* state of the ν_{11} out-of-plane rocking mode which is probably hybridized with the $(437)^{gr}$ *A* ground-state level [10]. With exclusion of these origins, our curves in effect represent deperturbed energies, which is why our fitted value of 8.273 cm^{-1} for the ν_8 *A-E* splitting in Table II is smaller than the usual value of 9.022 cm^{-1} determined as the difference between observed $K=0$ CO-stretching substate origins [1].

For the $\nu_8+\nu_{11}$ combination band, since only four data points were available, we fixed the a_2^v constant to zero. The resulting fitted curves in Fig. 1(h) must be regarded as very preliminary, but nevertheless are strikingly similar to the inverted τ curves for the singly excited ν_{11} state in Fig. 1(d), supporting the vibrational assignment.

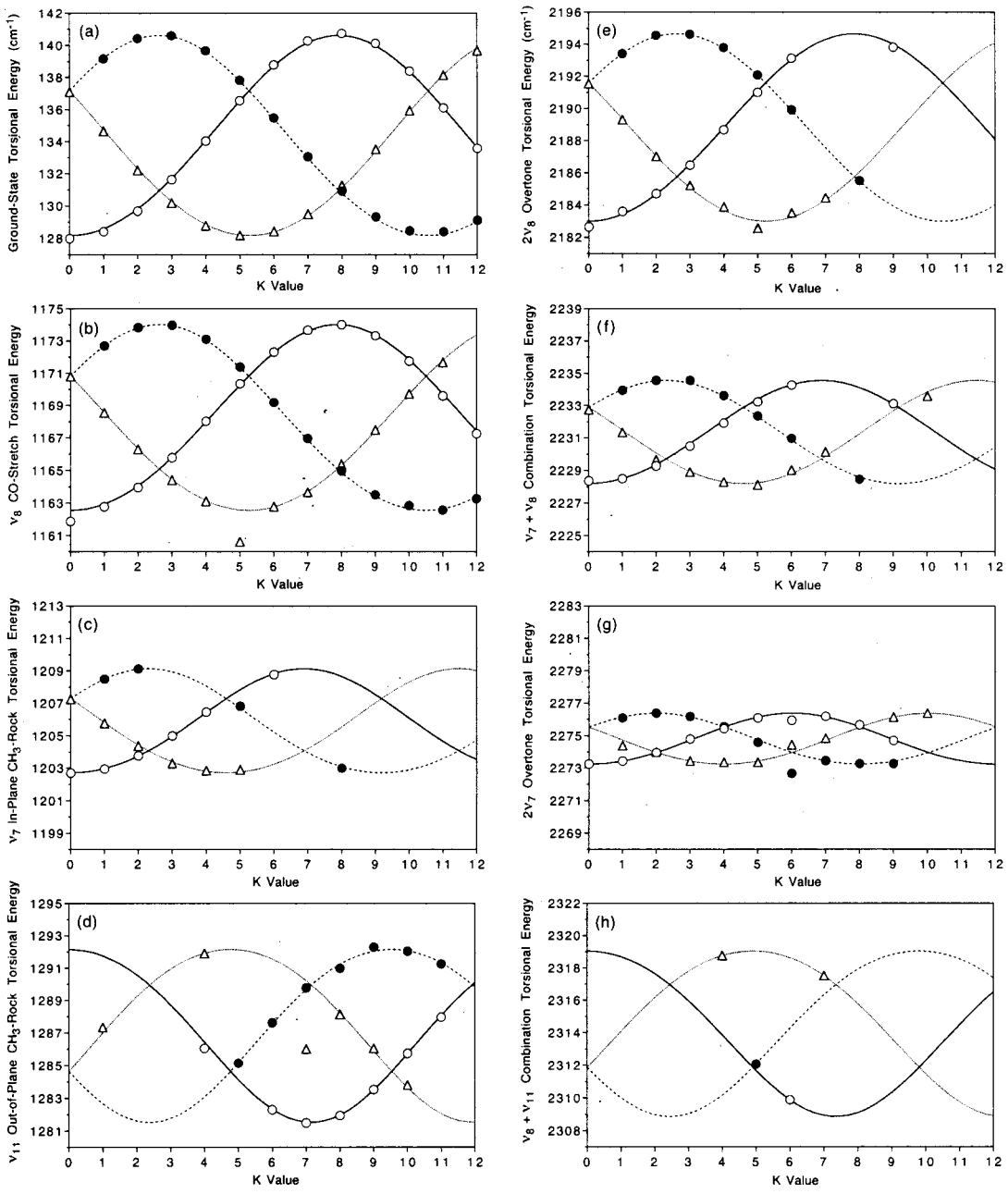

FIG. 1. CH_3OH τ curves of *K*-reduced torsional energies (in cm^{-1}) for (a) the ground vibrational state, (b) the ν_8 CO stretching mode, (c) the ν_7 in-plane CH_3 rocking mode, (d) the ν_{11} out-of-plane CH_3 rocking mode (from Ref. [10]), (e) the $2\nu_8$ CO-stretching overtone, (f) the $\nu_7+\nu_8$ combination, (g) the $2\nu_7$ CH_3-rocking overtone, and (h) the $\nu_8+\nu_{11}$ combination. Energies for $\tau=1$ are shown as open circles, $\tau=2$ as filled circles, and $\tau=3$ as triangles. The *K*-reduced energies were obtained by subtracting the *K*-rotational energy $[A-(B+C)/2]K^2$ from the substate origins. The continuous curves represent the fit of the substate origins to the five-parameter Fourier model, and are calculated with the constants from Table II.

V. APPLICATION OF THE $E\times E$ MODEL TO THE ν_7 AND ν_{11} TORSIONAL SPLITTING PATTERNS

In Table II, the *A*-*E* splitting decreases by approximately a factor of two in going from the ground state ($\nu_7=0$) to $\nu_7=1$, and by another factor of two in going to $\nu_7=2$. This trend is similar to that reported for the overtones of the ν_1 OH-stretching vibration [18], suggesting that this behavior is typical for methanol and may be expected for other modes such as the CH_3 bending vibrations. Although the amplitude and the periodicity both change for the ν_7 and $2\nu_7$ τ curves, the normal oscillatory patterns are still preserved in Figs. 1(c) and 1(g), so that in principle the curves could be interpreted according to the traditional one-dimensional torsional Hamiltonian in terms of effective torsional barrier heights $V_3^{\rm eff}$. However, the $K=0$ *A*-*E* splittings of 4.608 cm^{-1} for ν_7 and 2.290 cm^{-1} for $2\nu_7$ in Table II would correspond, keep-

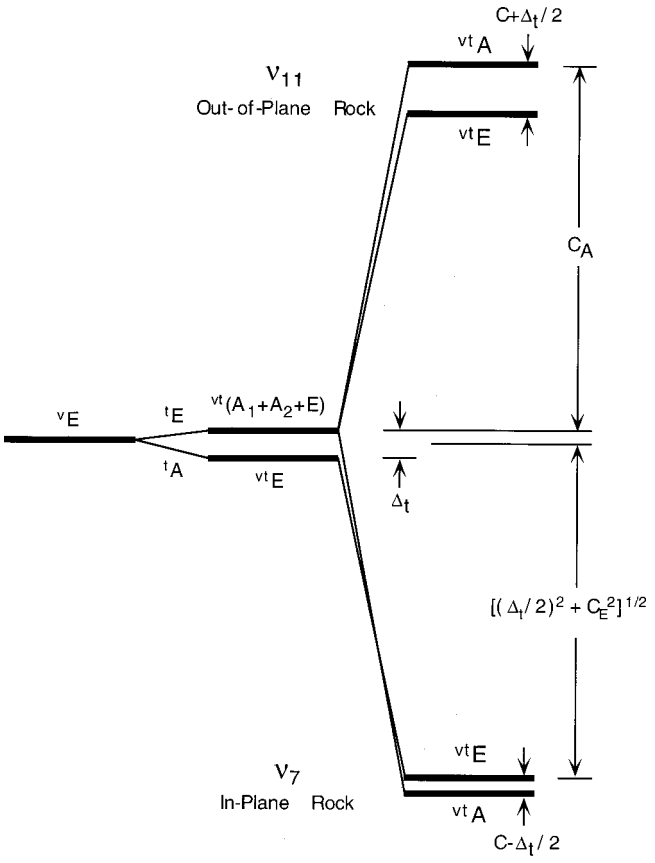

FIG. 2. Vibration-torsion energy level structure predicted for the $(n,K)=(0,0)$ levels of the ν_7 in-plane CH_3-rocking and ν_{11} out-of-plane CH_3-rocking modes of CH_3OH according to the $E\times E$ model of Ref. [12]. The initially degenerate $^{vt}A_1$ and $^{vt}A_2$ states are split by $\pm C_A$, and the coupled ^{vt}E states about their midpoint by $\pm[(\Delta_t 2)^2+C_E{}^2]^{1/2}$, where C_A and C_E are interaction parameters and Δ_t is the ground-state A-E torsional splitting. C_A and C_E are chosen to give a similar scale to that found experimentally and to reproduce the ν_7 A-E torsional splitting of $\sim\Delta_t/2$. The model predicts the upper inverted ν_{11} A-E splitting to be $-(C+\Delta_t/2)$ and the lower ν_7 splitting to be $(C-\Delta_t/2)$, where $C=C_A-[(\Delta_t/2)^2+C_E{}^2]^{1/2}\approx C_A-|C_E|$.

ing other parameters fixed at ground-state values, to $V_3^{\rm eff}$ values of 551.0 and 745.5 cm^{-1}, respectively, as compared to the ground-state value of 373.542 cm^{-1} [16]. If these changes were viewed according to the traditional power-series expansion in vibrational quantum number with the zero-point contribution of 1/2 included,

$$V_3^{\rm eff}=V_3^{\rm eq}+\Delta V_3(v_7+1/2) \tag{2}$$

where $V_3^{\rm eq}$ is the equilibrium value and ΔV_3 is the change per quantum of vibrational excitation, then we would obtain a zero-point correction of $\Delta V_3/2\approx 90\ cm^{-1}$ from the data of Table II, which seems unreasonably large. Coupled with the fact that the inversion of the A-E ordering for the ν_{11} and $\nu_8+\nu_{11}$ states is completely incompatible with the one-dimensional torsional Hamiltonian, it is clear that an alternative approach is required.

Previously, analogous inverted splittings for the ν_2 and ν_9 asymmetric CH stretching modes of CH_3OH were successfully explained by Wang and Perry [15] in terms of an internal coordinate 3×3 local-mode picture of three equivalent interacting CH bond stretches. In the present situation for the two-dimensional CH_3 rocking case, the new $E\times E$ vibration-torsion model proposed by Hougen [12] is applicable and provides a prescription for interrelating the A and E energies of the pair of E-like rocking vibrations of the molecule.

In the $E\times E$ model, one starts in the absence of interactions with a twofold degenerate ^vE vibrational mode of energy E_v. Torsional ^tA and ^tE energies are given by the usual one-dimensional Hamiltonian with a splitting of Δ_t about the center of gravity, so that $E(^tE)=+\Delta_t/3$ and $E(^tA)=-2\Delta_t/3$. (The torsional zero-point energy is implicitly included in E_v.) However, coupled vibration-torsion basis functions $|^{vt}\Psi\rangle$ are employed, taken as linear combinations of products $|^v\Psi\rangle|^t\Psi\rangle$ of $^vE_\pm$ vibrational functions with ^tA_t or $^tE_\pm$ torsional functions under the G_6 molecular symmetry group. This gives six $|^{vt}\Psi\rangle$ vibration-torsion basis functions $(^{vt}A_1+{}^{vt}A_2+2{}^{vt}E_\pm)$ for $n=0$, and represents the case of Fig. 1(c) in Ref. [12] with one threefold level $(^{vt}A_1+{}^{vt}A_2+{}^{vt}E)$ at energy $E_v+\Delta_t/3$ separated by the torsional splitting from a single lower level (^{vt}E) at $E_v-2\Delta_t/3$. Cubic interaction terms of $^{vt}A_1$ symmetry are then introduced involving operators $e^{i\gamma}Q_+^2$ and $e^{-2i\gamma}Q_+^2$, where γ is the angle of internal rotation. These terms split the degeneracy of the $^{vt}A_1$ and $^{vt}A_2$ states, and mix and further separate the two ^{vt}E states to give four vibration-torsion energy levels of the form

$$E(^{vt}A)=E_v+\Delta_t/3\pm C_A, \tag{3a}$$

$$E(^{vt}E)=E_v-\Delta_t/6\pm[(\Delta_t/2)^2+C_E^2]^{1/2} \tag{3b}$$

where the interaction parameters C_A and C_E involve products of torsion-vibration interaction constants and the matrix elements of the torsional and vibrational interaction operators. A wide variety of splitting patterns is then possible depending on the relative magnitudes of C_A and C_E, but at least one of the A-E pairs must be inverted with the ^{vt}A state lying above the ^{vt}E state.

The present application to the pair of CH_3 rocking states is illustrated in Fig. 2, with the A and E $(n,K)=(0,0)$ substate origins for the higher out-of-plane mode ν_{11} given by the $+$ signs in Eqs. (3), and those for the lower in-plane mode ν_7 by the $-$ signs. Figure 2 is drawn to agree qualitatively with our experimental findings, with a reduced splitting for the lower state and an inverted splitting for the upper. Now from Eqs. (3), the upper and lower splittings are $-(C+\Delta_t/2)$ and $(C-\Delta_t/2)$, where $C=C_A-[(\Delta_t/2)^2+C_E^2]^{1/2}\approx C_A-|C_E|$, giving Hougen's sum rule [12] that the sum of the splittings should equal $-\Delta_t$. However, our fitted splittings in Table II are -7.505 and 4.608 cm^{-1} for upper- and lower-rocking states, respectively, while the ground-state splitting Δ_t is 9.122 cm^{-1} [1]. Thus, while the $E\times E$ model in Fig. 2 clearly captures the essential physics of the situation, there are some differences in detail from our results.

If we estimate that $C\approx\Delta_t$ on the basis of the lower-state splitting in Fig. 2, then our fitted ^{vt}A and ^{vt}E $K=0$ origins of

1292.147 and 1284.642 cm^{-1} for the inverted ν_{11} curves in Fig. 1(d) and 1202.837 and 1207.445 cm^{-1} for the ν_7 curves in Fig. 1(c) give approximate values $C_A \approx |C_E| \approx 40\ cm^{-1}$. Comparison of Eqs. (3) above with Eqs. (10) of Ref. [12] shows that $C_A=(k_1t_3+k_2t_4)h$ and $C_E=(k_1t_1+k_2t_2)h$, where k_1 and k_2 are the interaction constants multiplying the $e^{i\gamma}Q_+^2$ and $e^{-2i\gamma}Q_+^2$ operators, the t_i are torsional matrix elements, and h is the vibrational matrix element $\langle {}^vE_+|Q_+^2|{}^vE_-\rangle$. The torsional matrix elements can be calculated using our ground-state eigenfunctions, with the following results for the $K=0$, $n=0$ elements:

$$t_1=\langle {}^tE_+|e^{+i\gamma}|{}^tA_1\rangle=0.959,$$

$$t_2=\langle {}^tE_+|e^{-2i\gamma}|{}^tA_1\rangle=0.741,$$

$$t_3=\langle {}^tE_+|e^{-i\gamma}|{}^tE_-\rangle=0.897,$$

$$t_4=\langle {}^tE_+|e^{-2i\gamma}|{}^tE_-\rangle=0.863.$$

Then, since $C>0$ from our results, we have the following condition:

$$C \approx C_A-|C_E|=[k_1(t_3-t_1)+k_2(t_4-t_2)]h$$
$$=[-0.062k_1+0.122k_2]h>0. \quad (4)$$

Assuming that $h>0$, this then implies that $k_2>k_1/2$, so that the two interaction terms appear to be of comparable magnitudes.

In general, although there are still some significant questions of detail, the $E\times E$ model does successfully rationalize the inverted splitting for ν_{11} and the greatly reduced splitting for ν_7 within the context of the traditional torsional Hamiltonian. Given that the in-plane and out-of-plane CH_3 rocking motions may well interact differently with the methanol OH group and thereby truly have different torsional barriers and vibrational energies, it would be interesting to examine the consequences of relaxing the constrains that the two modes be vibrationally and torsionally degenerate before the interactions are added, to see whether this might account for the discrepancies between the observed relative torsional splittings and the predictions of the model.

VI. DISCUSSION AND CONCLUSIONS

This paper presents a comparative picture of the torsion-vibration energy structures for eight states of CH_3OH involving excitation of the ν_7 (A' in-plane CH_3 rocking), ν_8 (A' CO stretching) and/or ν_{11} (A'' out-of-plane CH_3 rocking) vibrational modes, including the ground state. Assignments are reported for the $2\nu_7$ overtone, plus four perpendicular subbands for the $\nu_8+\nu_{11}$ combination band. For these two states plus the six states previously known, we obtained substate origins by expanding the excited-state energy term values as $J(J+1)$ power series. The origins were then fitted for the eight vibrational states to a simple five-parameter Fourier model to look for systematic trends in the energy structures and molecular parameters. *K*-reduced torsion-vibration energies were evaluated from the results of the Fourier fits, and plotted in τ-curves to display the excited-state torsional energy patterns.

The most striking features of the results in Table II and Fig. 1 are the rapid decrease in the *A-E* torsional splitting for the ν_7 in-plane CH_3 rocking mode, by about a factor of two per quantum of vibrational excitation, and the inverted *A-E* splitting for the ν_{11} out-of-plane CH_3 rock. The observed pattern for the $K=0$ energies of the two fundamental modes is discussed from the perspective of Hougen's recent $E\times E$ model of vibration-torsion energy structure for vibrations of degenerate *E* parentage [12]. Our experimental energy-level pattern is in overall qualitative agreement with the predictions from this model, but there are some differences of detail in the relative *A-E* splittings. Our results indicate that the two vibration-torsion interaction terms introduced in the $E\times E$ model are of comparable magnitude for CH_3OH.

Another notable feature of the results in Table II and Fig. 1 is the close parallel between the parameters of the singly excited rocking modes and those of the combination states with the CO stretch, both for the ν_7 and $\nu_7+\nu_8$ pair and the ν_{11} and $\nu_8+\nu_{11}$ pair. For the $\nu_8+\nu_{11}$ state, with just four data points, the energy curves are clearly very preliminary but the pattern from the Fourier fit is remarkably similar to that of the ν_{11} state, with an almost identical inverted torsional splitting. Thus, excitation of the CO stretching appears to influence neither the *A-E* splittings nor the ρ parameters for the CH_3 rocking modes to any great extent. The ν_8 mode acts simply as a chromophore in generating and lending intensity to the rocking combination bands but does not significantly perturb the torsional structure. This is useful in permitting a more complete mapping of the pattern of the in-plane rocking mode energy manifold in Fig. 1(f), since a number of substates seen in the $\nu_7+\nu_8$ combination band have not yet been identified for the weak ν_7 fundamental.

A further significant trend in Table II is the consistent and substantial decrease in the ρ parameter of about 0.030 per quantum of ν_7 excitation in going from state $\nu_7=0$ to $\nu_7=1$ to $\nu_7=2$ [i.e., from Figs. 1(a) to 1(c) to 1(g)]. This approximately linear decrease in ρ implies a zero-point correction of $\Delta\rho\approx 0.015$ for ν_7, while for ν_{11} the correction would be about 0.010. Comparable decreases in ρ occur for the ν_2 and ν_9 CH stretching modes according to the energy τ curves in Fig. 1 of Ref. [15], giving a sizeable total of $\Delta\rho/\rho\approx 6\%$ for the four methyl-group vibrations. If this change were ascribed solely to variation in the methyl moment I_{CH_3}, one would obtain $\Delta I_{CH_3}/I_{CH_3}\approx(1-\rho)^{-1}\Delta\rho/\rho \approx 32\%$. We should note also in this connection that higher-order terms in the Hamiltonian involving a KP_γ torsional operator, where P_γ is the torsional angular momentum, could contribute to an apparent variation in ρ [16,19], although these effects should be relatively small.

The methyl-group moment of inertia has traditionally been a difficult molecular parameter to isolate and evaluate spectroscopically. Our present results suggest that even in the favorable case of CH_3OH, the possibility of significant zero-point contribution to the ground-state effective parameters leads to considerable uncertainty about the equilibrium value of I_{CH_3} and consequently about the precise CH_3-group struc-

ture within the molecular environment. It is evidently important, as Hougen notes in his conclusion [12], to investigate extension of his $E \times E$ model to include the K dependence of the energies in order to explore whether changes in apparent ρ values might be produced by torsion-vibration interactions. Furthermore, it is likely that the still problematic question of exactly how to treat a distorted CH_3 group of nonthreefold symmetry in the torsion-vibration Hamiltonian will have to be solved before the vibrational ρ changes in Table II can be confidently linked to specific structural zero-point effects. In any event, it is clear from the variations among the parameters in Table II that good data on all of the vibrational fundamentals of CH_3OH (and ideally their overtones also) will be needed to permit reliable extrapolation to equilibrium values.

In general, with the evolving state of the art both in experimental techniques and in theoretical *ab initio* capabilities, we can be optimistic that a convergence of approaches will give new insights for molecules with large-amplitude internal motions. Current quantum chemical programs now allow the energy and structural variations accompanying changes in a particular molecular vibrational coordinate to be calculated, so that one can in principle determine the effects of vibrational averaging over that coordinate [20]. Experimentally, with resolution of the torsion-rotation structure in both fundamental and overtone bands of a given vibrational mode, the values of the molecular parameters can be probed at significantly different levels of excitation [18]. Thus, we may hope by comparing such theoretical and experimental results to develop more detailed pictures of the molecular multidimensional potential surface, a clearer view of the coupling among the small-amplitude vibrations and large-amplitude internal motions, and a better perspective on zero-point effects and their implications for molecular structural determinations.

ACKNOWLEDGMENTS

Two of us (R.M.L. and L.H.X.) acknowledge financial support for this research from the Natural Sciences and Engineering Research Council of Canada. We are grateful to J. T. Hougen for his interest and encouragement in this project, and for numerous stimulating discussions.

[1] G. Moruzzi, B. P. Winnewisser, M. Winnewisser, I. Mukhopadhyay, and F. Strumia, *Microwave, Infrared and Laser Transitions of Methanol: Atlas of Assigned Lines from 0 to 1258* cm^{-1} (CRC Press, Boca Raton, Florida, 1995).
[2] I. Mukhopadhyay, I. Ozier, and R. M. Lees, J. Chem. Phys. **93**, 7049 (1990).
[3] Li-Hong Xu, A. M. Andrews, and G. T. Fraser, J. Chem. Phys. **103**, 14 (1995).
[4] I. Mukhopadhyay, Spectrochim. Acta, Part A **54**, 1381 (1998).
[5] R. M. Lees, M. Mollabashi, L.-H. Xu, M. Abbouti Temsamani, M. Lock, and B. P. Winnewisser, Chem. Phys. Lett. **347**, 383 (2001).
[6] R. M. Lees, Li-Hong Xu, D. Hurtmans, and Z. Lu, in *52nd International Symposium on Molecular Spectroscopy* (Columbus, Ohio, 1997), Paper WF04.
[7] Li-Hong Xu, R. M. Lees, J. W. C. Johns, and S. Klee, J. Mol. Spectrosc. **162**, 397 (1993).
[8] S. Zhao, R. M. Lees, J. W. C. Johns, C. P. Chan, and M. C. L. Gerry, J. Mol. Spectrosc. **172**, 153 (1995).
[9] A. Predoi, R. M. Lees, and J. W. C. Johns, J. Chem. Phys. **107**, 1765 (1997).
[10] R. M. Lees and Li-Hong Xu, Phys. Rev. Lett. **84**, 3815 (2000).
[11] C. C. Lin and J. D. Swalen, Rev. Mod. Phys. **31**, 841 (1969).
[12] J. T. Hougen, J. Mol. Spectrosc. **207**, 60 (2001).
[13] T. George, W. Urban, and A. Le Floch, J. Mol. Spectrosc. **165**, 500 (1994).
[14] D. G. Burkhard and D. M. Dennison, J. Mol. Spectrosc. **3**, 299 (1959).
[15] X. Wang and D. S. Perry, J. Chem. Phys. **109**, 10795 (1998).
[16] Li-Hong Xu and J. T. Hougen, J. Mol. Spectrosc. **173**, 540 (1995).
[17] W. H. Weber and P. D. Maker, J. Mol. Spectrosc. **93**, 131 (1982).
[18] O. V. Boyarkin, T. R. Rizzo, and D. S. Perry, J. Chem. Phys. **110**, 11 359 (1999).
[19] R. M. Lees, J. Mol. Spectrosc. **33**, 124 (1970).
[20] M. Abbouti Temsamani, Li-Hong Xu, and D. S. Perry, Can. J. Phys. **79**, 435 (2001).